perimental data. In adenine the predicted wavelengths are always within 7 nm of the experimental peaks. Electron donation by the C-8 amino group shifts the longest wavelength peaks to longer wavelengths according to theory and in accord with the data on the related 8-methoxyadenine.[6] A detailed analysis of the configuration interaction matrix indicates that all those states quoted are essentially totally transitions.

Guanines. Table VI lists some results on guanine and 8-aminoguanine. The amino group again red shifts the longest wavelength absorption. The agreement between predicted and experimental results is not as good as in adenines, yet infinitely better than without CI. All the listed absorptions are predicted to be of the $\pi \rightarrow \pi^*$ type transitions again principally. In defense of the method one should emphasize that even subtle features such as the long wavelength shoulder in adenine (near 275 nm) are implied by the calculations.

This author feels that even the limited CI calculation reproduces the qualitative features of the uv spectra respectably and is thus of considerable value when one wants to interpret the spectra of molecules for which the transitions are not well defined.

Conclusions

Apparently ground-state trends are better predicted with the CNDO/2 method than excited-state properties. While use has already been made of the present series of substituents by others as well as the author's group, these series could be employed in a variety of other ways also. For example, in studying the theoretical origins of hydrogen bonding and stacking interactions one could compare the thermodynamics of self-association of adenosine and 8-bromoadenosine (or corresponding nucleotides). 8-Bromoadenine appears to have a very small dipole moment compared to adenine, whereas the C–Br bond, of course, is much more polarizable than the C–H bond. This would provide a handle on sorting out dipole–dipole interactions from induced dipole types (such as dispersion and dipole–induced dipole type), the latter mainly influenced by polarizability.

Considerable experimental work remains to be performed on the definition of proton and metal binding sites in the DNA bases. The theoretical definition is still lacking also, since there is not yet any unified theory correctly predicting protonation and metal binding sites on *all* bases simultaneously.

Finally, with the advent of volatile purine derivatives it would be fascinating to see whether or not the gas-phase proton affinities of these molecules follow the order of basicities found in aqueous medium.

Acknowledgment. Computer time was generously donated by the Rutgers University Center for Computer and Information Services. Thanks are due to the Rutgers University Research Council for financial support of the experimental work and to Mr. Hagay Niv for communicating his preliminary data.

Importance of Solvent Cohesion and Structure in Solvent Effects on Binding Site Probes

Richard L. Reeves,* Mary S. Maggio, and Lorenzo F. Costa

Contribution from the Research Laboratories, Eastman Kodak Company, and Kodak Park Division, Eastman Kodak Company, Rochester, New York 14650.
Received March 14, 1974

Abstract: The solvent effect on the corrected emission frequency of the fluorescent probe, 2-toluidinonaphthalene-6-sulfonate (TNS), and on the free energy of tautomerization of the dye probe, 4-phenylazo-1-naphthol-2,4′-disulfonate (PND), has been studied using a wide range of nonpolar, dipolar aprotic, and hydrogen-bonding solvents. There is good correlation between $\bar{\nu}_{max}$ for TNS and ΔG° for PND in hydrogen-bonding solvents, showing that the transition energy and free energy of the respective probes are subject to similar solvation effects. $\bar{\nu}_{max}$ for TNS in solvents covering a range of dielectric constants from 2.2 to 182.4 is correlated poorly by ϵ and by several empirical polarity scales but is correlated well by the solubility parameter, δ. ΔG° for the tautomerization of PND is also correlated by δ and by the solvent surface tension in water and low-molecular-weight amides and alcohols. The results indicate that specific polar or hydrogen-bonding interactions between solvent and probe make a smaller contribution to the solvent effects than the work of cavity formation in the solvents. It is suggested that the spectral changes that accompany binding to a macromolecule from aqueous solution result as much from loss of aqueous solvation characteristic of structured bulk water as from changes in polarity of the microenvironment.

The purpose of this study was to assess the importance of various solvent parameters that contribute to the effect of solvents on binding site probes and to solvatochromic effects in general. Dyes and fluorescent probes are commonly used to investigate the binding of organic ions to macromolecules and to gain insight into the nature of binding sites. Their utility results from the fact that the absorption curves, emission frequencies, or fluorescent quantum yields are significantly different in the bound state from the properties in aqueous solution. Since the spectral changes that accompany binding can be duplicated by transfer to organic solvents or by addition of polar organic solvents to aqueous solutions of the probes, efforts have

been made to relate microenvironment polarity in the binding site to solvent polarity.[1-6] Solvent polarity has been measured either by the usual dielectric functions or by empirical polarity scales.[7-9] Although there are examples in the literature that show good correlation of spectral properties of probes with solvent polarity, there are also cases where solvent properties other than polarity appear to play an important role. This is particularly true if a wide range of different solvents is considered. Correct conclusions about binding sites can only be reached if they are based on the correct premises regarding solvent effects on the probes.

Results from our laboratory indicate that several properties of ionic dyes that reflect solvation changes seem to depend as much on solvent structure as on polarity in water, amides, alcohols, and aqueous alcohols. These properties include specific hydrogen-bonding interactions,[10] spectral shifts,[11] changes in oscillator strength,[11] kinetic effects,[11] and tautomeric equilibria.[12] The importance of solvent cohesion in solvent effects on hydrophobic solutes was emphasized in a theory proposed recently by Sinanoglu.[13] In his treatment, the solvation free energy is the sum of all polar interactions, nonbonded attractions and repulsions, and the work required to make a solvent cavity to accommodate the solute. The surface energy of the microscopic cavity was related to the macroscopic surface tension, neglecting curvature corrections at molecular dimensions. The derived free energy for transfer of molecule A from solution to the gas phase was given by eq 1 where μ_A and v_A are the dipole moment and

$$\Delta G^{\circ}_A \approx a + b\mu_A^2/v_A - cv_A^{2/3}\gamma_1 - RT \ln kT/v_1 + \ldots \quad (1)$$

molecular volume of solute A, and γ_1 and v_1 are the macroscopic surface tension and molecular volume of the solvent. The coefficients a, b, and c contain, among other things, the refractive index function, $(n^2 - 1)/(n^2 + 2)$, and the dielectric function from the Onsager reaction field, $2(\epsilon - 1)/(2\epsilon + 1)$. Since these functions do not vary by much in a series of polar solvents, a, b, and c were treated as constants as a first approximation. By this model, ΔG°_A should show a linear dependence on γ_1 and a complex dependence on v_A in polar solvents. As v_A increases relative to v_1, the surface term, $v_A^{2/3}\gamma_1$, should dominate and become most important in water. The treatment separates the opposing solvent effects of positive interaction forces and negative surface or solvophobic forces.

In the present work we have attempted to test the relative importance of solvent polarity and cohesion in a detailed study of the effects of polar solvents on the emission frequencies of 2-toluidinonaphthalene-6-sulfonate (TNS) and on the solvent-sensitive tautomeric equilibrium of the azo dye, 4-phenylazo-1-naphthol-2,-4′-disulfonate (PND). The fluorescent indicator is well known as a probe for protein binding.[1,5,6] The azo dye is a useful probe since it binds to bovine serum albumin and to polyvinylpyrrolidone and interacts with cationic surfactants with accompanying shifts from the hydrazone tautomer, typical of aqueous microenvironments, to the azo tautomer in nonaqueous environments.[14] We have studied solvent effects on these probes dissolved in a wide range of dipolar aprotic and protic solvents, varying in dielectric constant from 2.2 to 182.4, and in several aqueous binaries.

Our earlier study of the tautomerization of azo dyes was limited to mixtures of similar solvents, since we had to calculate tautomer ratios from absorptivities and had to assume that medium effects on the absorptivities of the individual tautomers were small compared to the effects on the tautomer ratios.[12] Our inability to separate solvent effects on band shapes and positions from those on tautomer concentrations precluded a study of a wide variety of solvents. Qualitatively, however, it was apparent that the position of the tautomeric equilibrium was more sensitive to the hydrogen-bonded solvent structure than to dielectric properties. The recent development of a mathematical method for separating the effect of medium on band shape from the effect on concentration changes[10,15] now allows us to measure solvent effects on the equilibrium constants with confidence.

Experimental Section

Materials. TNS was Eastman reagent grade and was recrystallized as the sodium salt from aqueous sulfite–bisulfite solutions[1] until thin-layer chromatography on silica gel gave a single spot with two solvent systems [*n*-butyl alcohol saturated with 3% ammonia and 50% (v/v) ethanol–ethyl acetate]. PND was the material used previously.[12] Burdick and Jackson dioxane (distilled in glass and stored under nitrogen) was used immediately on opening without further purification. Dimethylformamide (Burdick and Jackson, "distilled in glass" and dried over sieves), ethylene glycol (Matheson Coleman and Bell chromatoquality reagent), methanol (Eastman spectro grade), and "absolute" ethanol were used as received. The remaining solvents were the best commercial grades available and were fractionated immediately before use; all boiled within a 1° range. Propylene carbonate and all the amides were dried over sieves before and after distillation.

Weighed samples of the indicators were dissolved directly into the pure solvents. Binary solvent mixtures were prepared by weight. Aliquots of aqueous stock solutions of the indicators were diluted at 25° with aqueous organic mixtures of known density and composition and the compositions were corrected for the added water. The aqueous pK_a of the OH group in PND is 7.4; the stock solution of this indicator was prepared in 0.001 M hydrochloric acid. The presence of absorption due to the phenolate of PND in the pure solvents was checked by acidification with a drop of 96% sulfuric acid. The weak acid ionization could only be detected in methanol; the tautomer ratio in this solvent was determined in the acidified solution.

Spectral Measurements. Absorption measurements were made

(1) D. C. Turner and L. Brand, *Biochemistry*, 7, 3381 (1968).
(2) C. J. Seliskar and L. Brand, *J. Amer. Chem. Soc.*, **93**, 5414 (1971).
(3) C. E. Williamson and A. H. Corwin, *J. Colloid Interface Sci.*, **38**, 567 (1972).
(4) C. E. Williamson and A. H. Corwin, *J. Colloid Interface Sci.*, **38**, 577 (1972).
(5) W. O. McClure and G. M. Edelman, *Biochemistry*, **5**, 1908 (1966).
(6) G. M. Edelman and W. O. McClure, *Accounts Chem. Res.*, **1**, 65 (1968).
(7) C. Reichardt and K. Dimroth, *Fortschr. Chem. Forsch.*, **11**, 1 (1968).
(8) F. W. Fowler, A. R. Katritzky, and R. J. D. Rutherford, *J. Chem. Soc. B*, 460 (1971).
(9) E. M. Kosower, *J. Amer. Chem. Soc.*, **80**, 3253 (1958).
(10) R. L. Reeves, R. S. Kaiser, M. S. Maggio, E. A. Sylvestre, and W. H. Lawton, *Can. J. Chem.*, **51**, 628 (1973).
(11) R. L. Reeves and R. S. Kaiser in "Water Structure at the Water-Polymer Interface," H. H. G. Jellinek, Ed., Plenum Press, New York, N. Y., 1972, p 56.
(12) R. L. Reeves and R. S. Kaiser, *J. Org. Chem.*, **35**, 3670 (1970).
(13) O. Sinanoglu in "Molecular Associations in Biology," E. B. Pullman, Ed., Academic Press, New York, N. Y., 1967, p 427.
(14) R. L. Reeves, R. S. Kaiser, and H. W. Mark, *J. Colloid Interface Sci.*, **45**, 396 (1973).
(15) W. H. Lawton, E. A. Sylvestre, and M. S. Maggio, *Technometrics*, **14**, 513 (1972).

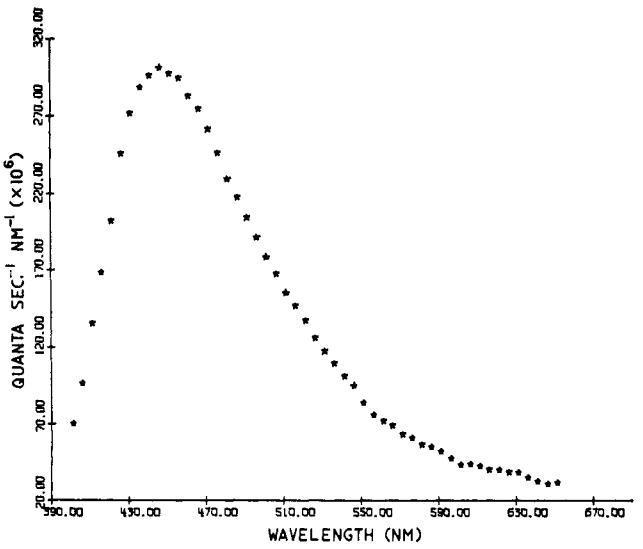

Figure 1. Corrected luminescence spectrum of TNS in 15 mol % *tert*-butyl alcohol in water.

on solutions of the sodium salt of PND on a Beckman DK-2A spectrophotometer. The wavelength calibration was checked periodically with a holmium oxide glass filter. Spectra were measured in 1-cm cells held in a thermostated cell block.

Luminescence spectra of TNS were measured on a prototype spectrofluorimeter described elsewhere.[16] Fluorescence was excited at 360 nm by an Osram XBO 150-W xenon source coupled with a Bausch and Lomb, Model 33-86-45, monochromator. The detection unit was a Beckman DK-2A spectroreflectometer equipped with a Hamamatzu R446S photomultiplier. The analog data were recorded on the Beckman recorder. The raw data were converted to digital form by reading the smoothed curves at 5-nm intervals into a Datex encoder and key-punching into IBM cards. The raw instrument measurements and calibration data were processed *via* a computer program written in Fortran IV language for the IBM System 360, whereby the raw data were corrected according to various instrument parameters. Corrected luminescence spectra were plotted off-line with a Calcomp plotter. A typical corrected spectrum is shown in Figure 1. The details of the calibration and correction procedure have been described.[16]

Analysis of Absorption Curves. We assumed that each experimental curve was a linear combination of two component functions. Thus, the ith curve can be modeled by

$$A_i(\lambda) = \theta_{1i} f_A\left(\frac{\lambda - \theta_{2i}}{\theta_{3i}}\right) + \theta_{1i} f_H\left(\frac{\lambda - \theta_{5i}}{\theta_{6i}}\right) + \text{error} \quad (2)$$

where A_i is the measured absorbance, θ_{1i} and θ_{4i} are the absorbances at the maxima, θ_{2i} and θ_{5i} are the respective wavelengths of maximum absorption, θ_{3i} and θ_{6i} are proportional to the bandwidths at half-peak height, and $f_A(\lambda)$ and $f_H(\lambda)$ are the shape functions for the respective tautomers. The details of the analysis are the same as given previously.[10,15] The shape function for the azo tautomer was determined from the absorption curve of PND in acetonitrile, where the hydrazone makes no contribution. Initially, we let the absorption curve of PND in water at 10° represent the shape function for pure hydrazone, according to our earlier estimate.[12] It was found, however, that the residual errors for resolution of families of curves in aqueous organic solvents were reduced slightly by assuming that the experimental curve in water at 10° contained only 97.5% hydrazone. The shape function for pure hydrazone was then constructed mathematically by a self-modeling method[15] from this experimental curve. With the final $f_i(\lambda)$ and eq 2, we could reproduce all experimental absorption curves with root-mean-square deviations that rarely exceeded 0.003 absorbance and that frequently were less than 0.002. A plot of a typical curve resolution is shown in Figure 2.

The tautomer ratios are proportional to the relative areas under

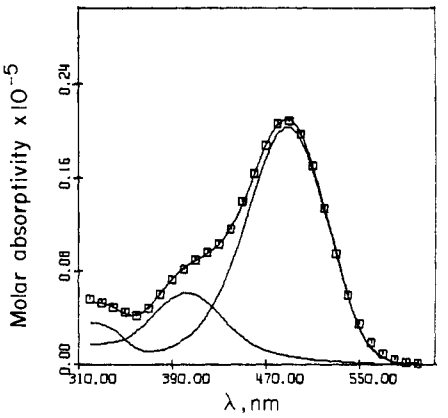

Figure 2. Resolved absorption curve of PND in formamide at 25°. The line through the data points is the summation of absorptivities of the component curves.

the resolved curves of the individual tautomers. The proportionality constant relating concentration and band intensity is defined by

$$k_A cl = I_A = \int_{\lambda_1}^{\lambda_n} \theta_1 f_A\left(\frac{\lambda - \theta_2}{\theta_3}\right) d\lambda \quad (3)$$

for the azo band, where λ_i is the wavelength in meters, c is the concentration in molarity, l is the solution thickness in meters, and k has units of l./mol. The intensities were computed as the product of the absorbances at the maxima, the bandwidths at half peak height, and the area under the normalized $f_A(\lambda)$ and $f_H(\lambda)$ rather than by integration between fixed wavelengths to allow for band shifts and band broadening and to ensure that areas were determined for the whole wavelength range for which the shape functions were defined. The tautomer ratio, K_T = [hydrazone]/[azo], is the ratio $I_H k_A / I_A k_H$. Although the individual k_i varied a little with solvent, we assumed that the ratio, k_A/k_H, was constant in various solvents.

Surface Tensions and Solubility Parameters. Surface tension values were taken from standard compilations. In cases where values were not listed at 25°, they were calculated using interpolation equations giving γ as a function of temperature[17] or were estimated by graphical interpolation. We measured the surface tension of 1,1,1-trifluoroethanol (TFE) at 23° using the Wilhelmy slide and a tensiometer. Values of the solubility parameters, δ, were taken from several compilations.[8,18,19] Where values were

$$\delta = ((\Delta H_V - RT)/V_M)^{1/2} \quad (4)$$

not listed or where listed values did not agree, values were calculated from eq 4 where ΔH_V is the enthalpy of vaporization of the liquid at 25° and V_M is the molar volume. ΔH_V for TFE and for 1,3-propanediol at 25° was estimated[18] from eq 5 where T_b is the boiling point at 760 mm in degrees Kelvin.

$$\Delta H_V = 27.3T_b + 0.020T_b^2 - 2950 \quad (5)$$

Results

We estimate the wavelengths of maximum emission of solutions of TNS are accurate to no more than ±2 nm in the best cases, since the corrected spectra were only plotted at 5-nm intervals. A larger error is estimated for solvents in which the quantum yield or solubility is low and the signal-to-noise ratio is correspondingly higher. Despite this limitation, our values agree well with those recorded by McClure and Edelman[5] using 12 solvents in which common measurements were made. The very weak luminescence of TNS in water made the direct measurement of $\bar{\nu}_{max}$ un-

(16) L. Costa, F. Grum, and D. J. Paine, *Appl. Opt.*, **8**, 1149 (1969).

(17) J. A. Riddick and W. B. Bunger, "Organic Solvents," Wiley-Interscience, New York, N. Y., 1970.

(18) J. Brandrup and E. H. Immergut, Ed., "Polymer Handbook," Interscience, New York, N. Y., 1966.

(19) L. H. Lee, *J. Paint Technol.*, **42**, 365 (1970).

Table I. Emission Maxima of TNS and Tautomer Ratios of PND in Various Solvents

Solvent	ϵ[a,b]	γ,[a,b] dyn/cm	δ,[c] (cal/cc)$^{1/2}$	λ_{max} (TNS), nm	K_T (PND)[a]
Ethyl acetate (EA)	6.02	23.0	9.1	411	
Dioxane (DIOX)	2.21	32.8	10.0	417	
Acetone (AC)	20.70	22.3	9.9	419	
Isopropyl alcohol (IPA)	19.92	20.2	11.5	422	
Dimethylacetamide (DMA)	37.78	33.3	10.8	423	
n-Butyl alcohol (NBA)	17.51	24.2[d]	11.4	424	
tert-Butyl alcohol (TBA)	12.47	20.0	10.0	426	
N,*N*-Dimethylformamide (DMF)	36.71	35.2	12.1	428	
Ethanol (E)	24.55	21.85[d]	12.7	429	0.019
Propylene carbonate (PC)	65.1[e]		13.3	435	
Benzyl alcohol (BA)	13.1[e]	39.5	12.1	442	
Methanol (M)	32.70	22.18[d]	14.5	444	0.046
N-Methylpropionamide (NMP)	172.2	31.7		448	0.048
1,3-Propanediol (13PD)	35.0[e]	45.2	13.3[f,g]	455	0.135
1,2-Propanediol (12PD)	32.0[e]	36.51	14.5[f]	455	0.093
Ethylene glycol (EG)	37.7	46.0	15.7[h]	462	0.226
Glycerol (GLY)	42.5	62.5	16.5[h]	463	0.943
N-Methylformamide (NMF)	182.4	38.9	16.1	464	0.196
Formamide (FA)	109.5	57.91	19.2	483	1.68
Trifluoroethanol (TFE)		20.4	10.8[f,g]	490	0.719
Water	78.39	71.81	23.4	515	8.3

[a] 25° except where noted. [b] Reference 17, except where noted. [c] Reference 8, except where noted. [d] From J. Timmermans, "Physico-chemical Constants of Pure Organic Compounds," Vol. I, Elsevier, New York, N. Y., 1950. [e] 20°. [f] Calculated from eq 3. [g] H_V calculated from eq 4. [h] Reference 19.

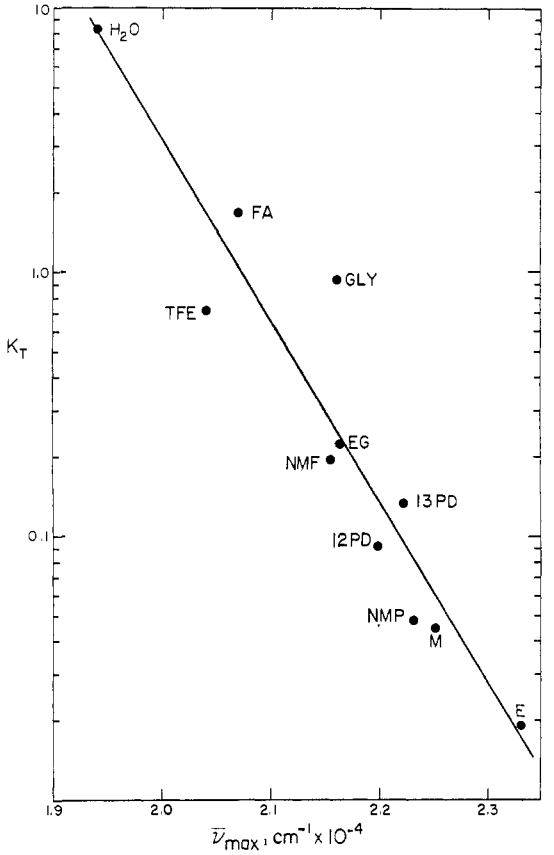

Figure 3. Correlation of log K_T for PND at 25° with $\bar{\nu}_{max}$ of TNS. The line is the least-squares line.

certain. A value of 2.00×10^4 cm^{-1} has been reported.[5] We obtain a value of 1.94×10^4 cm^{-1} as the average from linear extrapolations to zero mole fraction of plots of $\bar{\nu}_{max}$ *vs.* mole fraction of alcohol in water-rich aqueous ethanol and *tert*-butyl alcohol.

The spectra of PND obtained in non-hydrogen-bonding solvents gave no indication of measurable amounts of the hydrazone tautomer. In most hydrogen-bonding solvents, the intensity ratios of the resolved components fell in the measurable range from 0.04 to 20. The method of curve resolution gave precise values of K_T in the range of $0.05 < K_T < 5$. Thus, replicate determinations on different solutions gave $K_T = 0.196$ with a standard deviation of 0.005 in *N*-methylformamide, whereas four replicates in water at 25° gave $K_T = 8.70$ with a standard deviation of 1.90.

Changing solvents and temperature caused small but significant changes in absorptivity, bandwidth, and wavelength of the two component bands. This was also true with mixed aqueous solvents. We repeated our earlier measurements in ethanol–water and *tert*-butyl alcohol–water, for which we previously had assumed negligible medium effects on the band shapes.[12] The new results gave plots of log K_T *vs.* mole fraction of alcohol that are qualitatively the same as those obtained earlier, but the numerical values of K_T in the water-rich solutions are different. The least-squares fit of the corrected values is described by eq 6 and 7 for

$$K_T = 7.68 \exp(-21.9x_2) + 0.570 \exp(-4.57x_2) \quad (6)$$

$$K_T = 8.04 \exp(-47.6x_2) + 0.273 \exp(-3.24x_2) \quad (7)$$

ethanol–water and *tert*-butyl alcohol–water, respectively, where x_2 is the mole fraction of alcohol.

Table I lists the solvents, the emission maxima of TNS, the tautomer ratios of PND, and the solvent properties and parameters used in this study.

Figure 3 shows the relation between log K_T at 25° for PND and the $\bar{\nu}_{max}$ of TNS in 11 hydrogen-bonding solvents. The correlation coefficient, r, is 0.946. This plot shows that whatever is responsible for the observed solvent effects, the free energy of tautomerization for PND, $\Delta G_T°$, and the transition energy for TNS respond similarly in hydrogen-bonding solvents.

Figure 4 shows the frequency of the emission maximum of TNS as a function of the mole fraction of alcohol in *tert*-butyl alcohol–water and ethanol–water

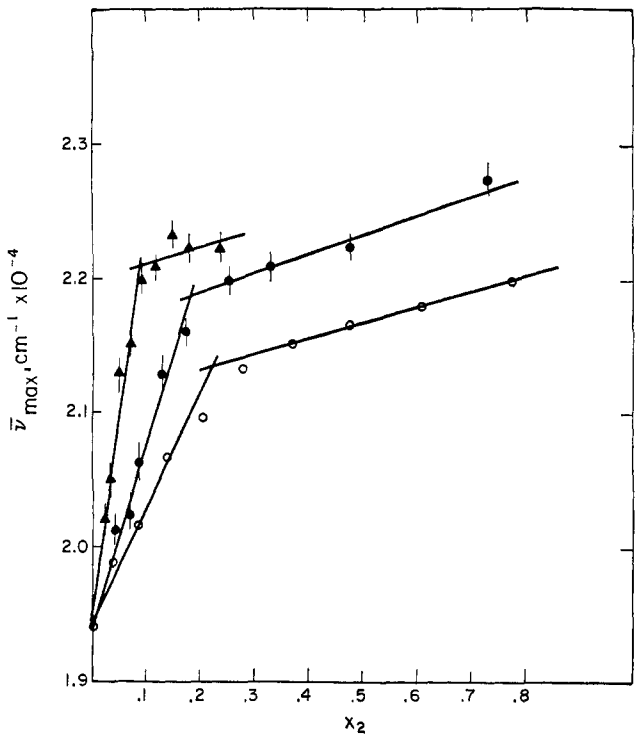

Figure 4. Plot of $\bar{\nu}_{max}$ of TNS in aqueous ethanol (●) and aqueous *tert*-butyl alcohol (▲) and of 1,7-ANS in aqueous ethanol (○) as a function of the mole fraction of alcohol.

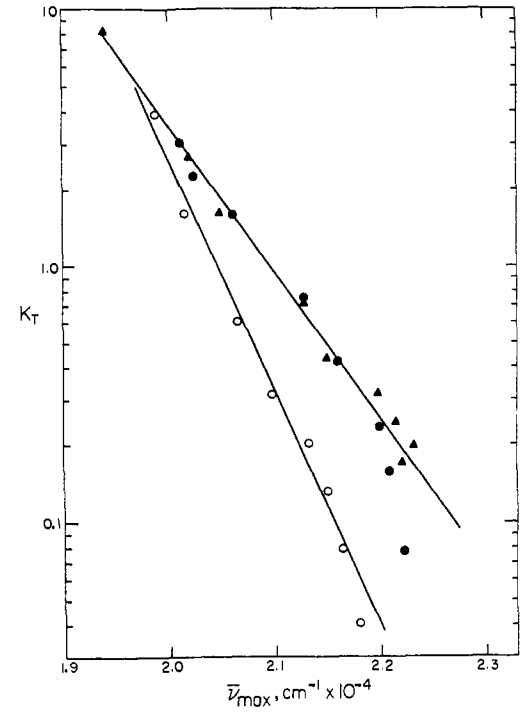

Figure 5. Correlation of log K_T for PND at 25° with $\bar{\nu}_{max}$ of TNS in aqueous ethanol (●) and aqueous *tert*-butyl alcohol (▲) and with $\bar{\nu}_{max}$ of 1,7-ANS in aqueous ethanol (○).

and of 1-anilinonaphthalene-7-sulfonate (1,7-ANS) in ethanol–water mixtures. The data for 1,7-ANS are those of Turner and Brand.[1] A similar plot is obtained with $\bar{\nu}_{max}$ of 2-anilinonaphthalene-6-sulfonate in ethanol–water.[2] The breaks in the plots occur at compositions where a number of other properties of the mixtures show extrema that are associated with changes in the hydrogen-bonded structure of the medium.[20–22] Plots of $\bar{\nu}_{max}$ for both probes as a function of the Kosower Z values show similar breaks, showing that solvent polarity as measured by this scale does not correlate $\bar{\nu}_{max}$, despite claims to the contrary.[1] A plot of $\bar{\nu}_{max}$ as a function of dielectric constant of the solvent mixtures is a curve with the data points for both mixtures falling on a common plot. We have shown previously that plots of $\Delta G°_T$ of PND in these alcohol–water mixtures show breaks similar to those of Figure 4 and at the same compositions.[12] This suggests that structural changes as well as polarity in the mixed solvents are affecting the transition energies of TNS and $\Delta G°_T$ of PND in a similar way. A plot of log K_T for PND as a function of $\bar{\nu}_{max}$ for TNS in these mixtures (Figure 5) confirms this conclusion. There is good correlation of log K_T with $\bar{\nu}_{max}$ up to 24 mol % *tert*-butyl alcohol (56 wt %) and 30 mol % ethanol (52 wt %) and with $\bar{\nu}_{max}$ of 1,7-ANS up to 48 mol % (70 wt %) ethanol. These ranges cover the compositions over which the major changes in K_T and $\bar{\nu}_{max}$ occur and over which the breaks in the plots of Figure 4 are found.

The poor correlation of $\bar{\nu}_{max}$ of TNS with dielectric constant in 20 pure solvents is seen from Figure 6. This parameter even fails to predict the correct direction of the shift in the most polar solvents. The dielectric function, $(\epsilon - 1)/(2\epsilon + 1)$, also failed to correlate the

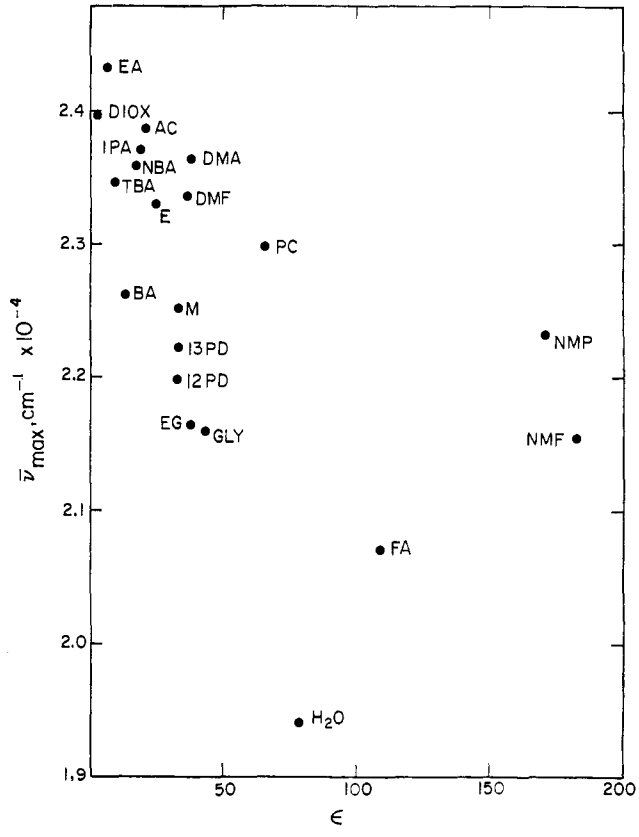

Figure 6. Plot of $\bar{\nu}_{max}$ of TNS as a function of the solvent dielectric constant. Solvent designations are given in Table I.

(20) F. Franks and D. J. G. Ives, *Quart. Rev., Chem. Soc.*, **20**, 1 (1966).
(21) F. Franks in "Physicochemical Processes in Mixed Aqueous Solvents," F. Franks, Ed., American Elsevier, New York, N. Y., 1967, p 50.
(22) E. M. Arnett, ref 21, p 105.

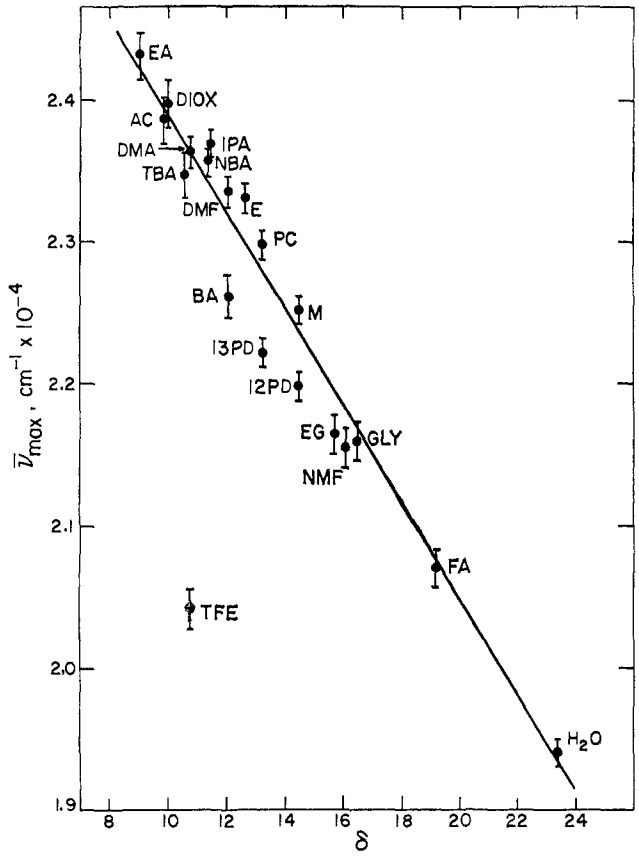

Figure 7. Plot of $\bar{\nu}_{max}$ of TNS as a function of the Hildebrand solubility parameter. The line is the least-squares line. Solvent designations are given in Table I.

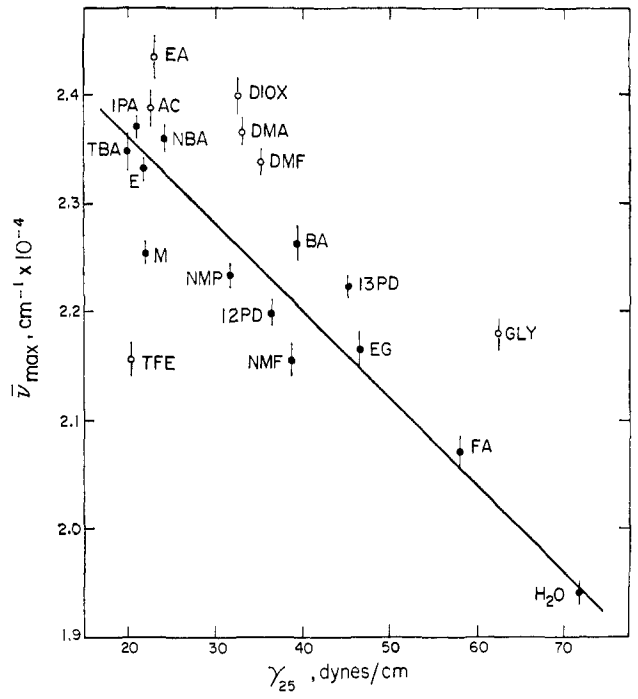

Figure 8. Plot of $\bar{\nu}_{max}$ of TNS as a function of solvent surface tension at 25°. The line is the least-squares line for the solvents plotted as closed circles. Solvent designations are given in Table I.

emission frequencies. Turner and Brand also found poor correlation of $\bar{\nu}_{max}$ of 1,7-ANS with dielectric properties of pure solvents. It was shown earlier that there is poor correlation between $\Delta G°_T$ of PND and ϵ in hydrogen-bonding solvents.

Figure 7 shows a plot of $\bar{\nu}_{max}$ for TNS as a function of the Hildebrand solubility parameter, δ,[23] in 20 solvents. This parameter is the square root of the cohesive energy density of the solvent (eq 4) which in turn is a measure of the total molecular cohesion per cubic centimeter of liquid. The solid line is the regression line omitting the point of TFE and is given by

$$\bar{\nu}_{max} = (2.739 \pm 0.026)10^4 - (0.0350 \pm 0.018)10^4\delta \quad (8)$$

The correlation coefficient is 0.977. The standard deviation from the regression line is 278 cm^{-1}, amounting to a predictive error of about 6 nm at 450 nm. The unusually large red shift in TFE is probably the result of specific hydrogen bonding since this solvent is a much stronger hydrogen-bond donor than other alcohols with similar bulk properties.[24,25]

The emission maximum of TNS is plotted as a function of the surface tension of 20 solvents in Figure 8 to test the Sinanoglu relationship. The overall correlation is poor. Most of the hydrogen-bonding solvents, including water, alcohols, primary and secondary amides, and the glycols, give fair correlation (r = 0.964). Glycerol and TFE are exceptions. The line in Figure 8 is the regression line for those hydrogen-bonding solvents plotted as solid circles.

The emission maximum is correlated poorly by the Kosower Z values[9] in 11 pure solvents (r = 0.812) and by the Reichardt and Dimroth E values[7] in 17 solvents (r = 0.850).

Values of log K_T for PND are plotted as a function of surface tension and δ in Figure 9. Trifluoroethanol is an anomalous solvent here also and appears to provide unusual stabilization of the hydrazone form of PND by a specific interaction that is not typical of other hydrogen-bonding solvents having similar bulk properties. With the exception of this solvent, $\Delta G°_T$ of PND is correlated fairly well by either surface tension (r = 0.964) or by the solubility parameter (r = 0.935). As can be seen from Table I, the solvent effect on $\Delta G°_T$ is not related directly to the solvent dielectric constant.

A further indication of the importance of solvent structure on the position of the tautomeric equilibrium of PND was sought by measuring K_T in dioxane–water mixtures. These mixtures have density and viscosity maxima at 30 and 25 mol % dioxane, respectively.[26] These extrema are probably associated with changes in solvent structure, although it is believed that dioxane does not cause the same enhancement of long-range order in the water-rich compositions as the alcohols.[21,26] Figure 10 shows that K_T has a minimum at 33 mol % dioxane, showing that the structural factors leading to extrema in the density and viscosity also affect the tautomerization of the dye solute. McClure and Edelman noted that the $\bar{\nu}_{max}$ for TNS also seemed to depend on solvent structure in dioxane-rich compositions of aqueous dioxane.[5] The dielectric constant decreases monotonically with increasing dioxane content.

(23) J. H. Hildebrand and R. L. Scott, "Regular Solutions," Prentice-Hall, Englewood Cliffs, N. J., 1962, pp 89–103.
(24) J. Figueras, *J. Amer. Chem. Soc.*, **93**, 3255 (1971).
(25) D. F. Evans and M. A. Matesich, *J. Solution Chem.*, **2**, 193 (1973).
(26) R. L. Kay and T. L. Broadwater, *Electrochim. Acta*, **16**, 667 (1971).

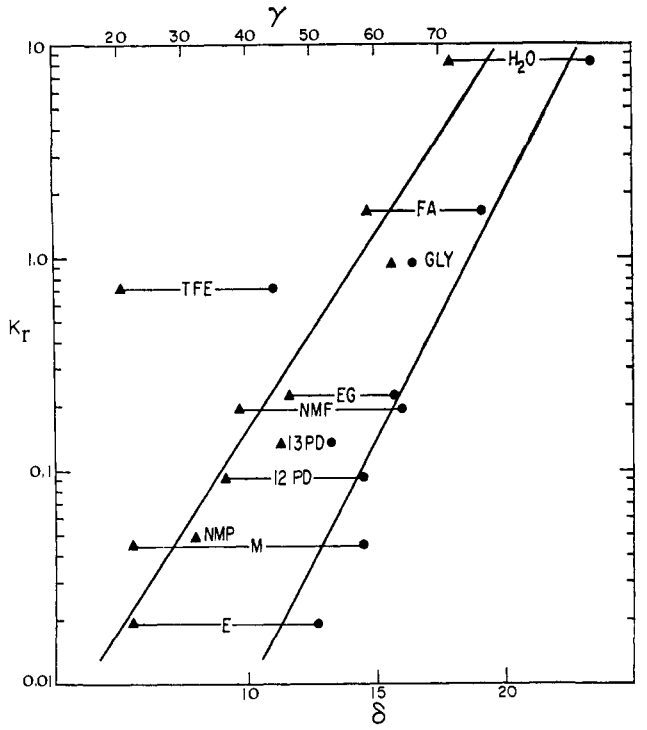

Figure 9. Semilog plot of K_T for PND at 25° as a function of δ (●, lower abscissa) and of surface tension (▲, upper abscissa). The lines are least-squares lines with the point for TFE omitted. Solvent designations are given in Table I.

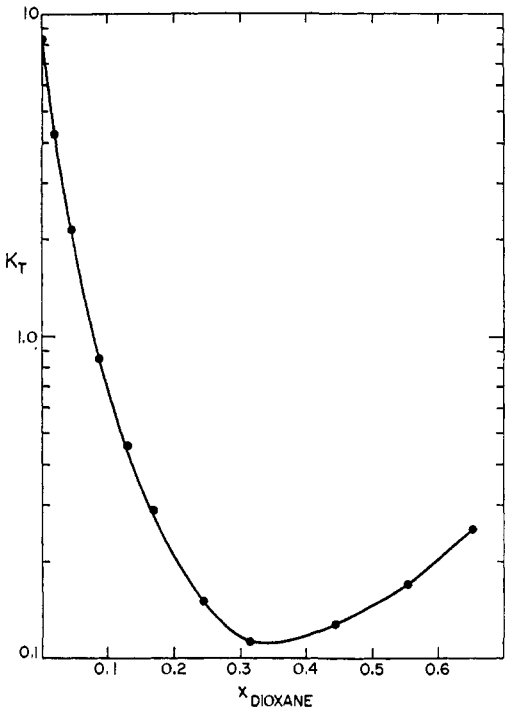

Figure 10. Semilog plot of K_T for PND at 25° as a function of the mole fraction of dioxane in aqueous dioxane.

Enthalpies and entropies of tautomerization of PND were computed from the temperature variation of K_T in eight pure solvents and in aqueous ethanol and *tert*-butyl alcohol. The temperature range was 4–40°. K_T values in water were too large to measure directly at lower temperatures, so values of log K_T were obtained at various temperatures by extrapolation to zero mole fraction of linear plots of log K_T *vs.* mole fraction in *tert*-butyl alcohol–water mixtures at mole fractions less than 0.05. The derived values of $\Delta H°$ and $\Delta S°$ are given in Table II. In our earlier attempt to determine these parameters in aqueous organic solvents,[12] we could not allow for the effects of temperature and changing medium on the component band shapes and therefore the previous values are somewhat in error. The present results show the same trends in the values in aqueous binaries that we noted earlier; *i.e.*, as organic solvent is added to water, the azo to hydrazone conversion becomes less exothermic and the entropy change becomes more favorable. The data for the pure solvents also show this trend in $\Delta H°$ and $\Delta S°$ in going from water, with three-dimensional structure, to methanol and *N*-methylformamide, which can only form linear chains. An excellent Barclay–Butler plot of $\Delta S°$ *vs.* $\Delta H°$ is obtained for the values found in water, formamide, ethylene glycol, and all the aqueous binaries. Somewhat more scatter is seen in values obtained in the other pure solvents. The slope of the linear plot is 380°K.

Table II. Solvent Effects on the Thermodynamic Parameters for the Azo to Hydrazone Tautomerization of PND at 25°

Solvent	x_2	$-\Delta H° \pm$ s, kcal/mol	$-\Delta S° \pm$ s, cal/(°K mol)
H_2O		9.40 ± 2.6	27.2 ± 9.2
FA		5.65 ± 0.30	18.0 ± 1.1
EG		2.22 ± 0.30	10.5 ± 1.1
NMF		3.33 ± 0.21	14.3 ± 0.7
13PD		2.10 ± 0.32	10.9 ± 1.2
12PD		2.21 ± 0.18	12.1 ± 0.6
TFE		1.47 ± 0.19	5.6 ± 0.7
M		1.46 ± 0.27	11.0 ± 1.0
E–H_2O	0.044	6.79 ± 0.48	20.2 ± 1.8
	0.088	5.97 ± 0.30	18.9 ± 1.1
	0.131	4.11 ± 0.13	14.2 ± 0.5
	0.254	1.45 ± 0.14	7.6 ± 0.5
TBA–H_2O	0.018	8.55 ± 0.24	25.7 ± 0.8
	0.035	6.88 ± 0.67	21.8 ± 2.4
	0.051	5.48 ± 0.10	18.5 ± 0.4
	0.094	1.05 ± 0.18	5.6 ± 0.6
	0.150	0.22 ± 0.26	3.9 ± 0.9
	0.306	0.10 ± 0.14	4.8 ± 0.5

Discussion

Solvent parameters related to solvent cohesion correlate the probe properties better than those related to solvent polarity, particularly in polar, hydrogen-bonded solvents. Both δ and γ are bulk solvent properties that are measured independently of any indicator and imply no specific or positive interaction with a solute. Correlation of probe properties with these parameters suggests that solvophobic or cavity surface forces play a more important role in altering the measured probe properties than positive interaction forces. Our results give little support to the hypothesis that the solvent effects studied here are caused mainly by changes in solvent polarity as measured by dielectric properties or by empirical scales. It follows that conclusions regarding the polarity of a binding site in a macromolecule that are based exclusively on such spectral data are also poorly founded. Certainly any efforts to obtain quantitative estimates of binding-site polarity would be suspect.

The results do not imply that polar interactions are not present. They show, however, that these interactions become largely saturated so that at high polarity and solvent cohesion, the solvophobic and structural effects become relatively more important. As an example, values of the dielectric function, $(\epsilon - 1)/(2\epsilon + 1)$, increase by less than 6% over a range of dielectric constants from 24.6 (ethanol) to 182.4 (NMF).

Our results support the Sinanoglu theory. The theory predicts that the best correlation with γ will be obtained with the smallest solvent molecules having the highest intermolecular cohesion, and this is found. Although Sinanoglu uses surface tension to measure cavity surface energy, δ may be a better empirical measure of this energy at molecular dimensions. Surface tension measures the energy required to overcome molecular cohesion in the bulk liquid in order to transfer molecules from the bulk to an uncurved air–liquid interface. δ and γ have been related empirically through the equation[27]

$$\delta = 4.1(\gamma/V_M^{1/3})^{0.43} \quad (9)$$

The two parameters are not linearly related so it would not be expected that data giving high correlation with one parameter would necessarily be correlated as well by the other. In addition, Lee has shown that only 65% of 129 polar and nonpolar liquids examined follows eq 9.[19]

All the measured properties fall at an extreme in water, the solvent with the greatest intermolecular cohesion and three-dimensional structure. The data suggest that the spectral changes that accompany the transfer of the probes from aqueous solution to hydrophobic binding sites result from loss of the aqueous solvation sheath that exists in bulk structured water around the probes. It is not necessarily a corollary that water molecules are absent in the site, although this may be the case. The binding site may be less polar than the aqueous microenvironment, but spectral changes of these probes provide poor evidence for this. If the microenvironment in the binding site is similar to the solvation sheath in *N*-methylformamide, the site could be more polar than the aqueous solution.

The concept of a solvent cavity is a useful one for theoretical treatments of solvation of solutes[13,28–30] although the application of bulk properties such as surface tension, which is defined for macroscopic surfaces, to such cavities may be questionable. The concept has been used successfully to relate the free energy of solution of gases and hydrocarbons in liquids. Hermann[28] has calculated the areas of the solvent cavities in water needed to accommodate a large number of hydrocarbons and has obtained good correlation between the logarithms of the solubilities and the calculated areas. The cavity areas are not trivial. The calculated cavity area for benzene is 241 Å^2 compared to a space of 12.7 Å^2 occupied by one water molecule in the cavity surface. The cavity requirement for the probes studied here will be much larger, although the structuring of the water at the "interface" will not be as uniform as for a hydrocarbon solute. The nonuniformity results from polar interactions between solvent and heteroatoms of the probes. Differences in these interactions among solvents are undoubtedly responsible for the lack of better correlation of the probe properties with solvent properties related to cohesive interactions.

In order for solvophobic contributions to the solvation energy of a solute to be manifested as a solvatochromic effect or as a shift in equilibrium between two solvated species, the two states involved must be able to respond differentially to changes in the cavity surface energy. It would not be expected, for instance, that differences in solvophobic contributions to solvation of a perfectly rigid dye molecule would contribute to a solvatochromic effect. We can speculate on why solvent cohesion contributes heavily to the observed solvent effects on the probes studied here. It has been suggested that coplanarity of the two rings in anilinonaphthalenesulfonates is necessary for fluorescence.[5,31] The fluorescence of anilinonaphthalenesulfonates is quenched in water whereas that of the corresponding aminonaphthalenesulfonates is not.[32] The quantum yield of TNS depends much more on solvent viscosity than that of the corresponding amino derivative.[5] This indicates that an important pathway for nonradiative loss of excitation energy in the anilinonaphthalenesulfonates is through internal rotation. The high surface energy of the cavity in water may be minimized in the equilibrium excited state when the rings of the anilinonaphthalenesulfonates are twisted out of coplanarity. Apparently, the greater the cavity surface energy, the greater is the twisting and the lowering of the excited-state energy on solvent and solute reorientation and the less is the energy gap between the equilibrium excited state and the Franck–Condon ground state. A red shift results. Support for this hypothesis comes from the fact that a red shift of the emission frequency of 2.6 kcal is obtained on transfer of 2-aminonaphthalene-6-sulfonate from ethanol to water, whereas a shift of 11.6 kcal results from the same transfer of 2-anilinonaphthalene-6-sulfonate.[2] If these suggestions are correct, the contribution to the frequency shift from solvent cohesion should be relatively small with the aminonaphthalenesulfonates compared to the anilinonaphthalenesulfonates. No data for a wide range of pure solvents are available to test this suggestion, although the frequency shift of 2-aminonaphthalene-6-sulfonate in aqueous ethanol is accounted for by consideration of solvent polarity alone.[2]

Similar arguments can be applied to the tautomeric equilibrium of PND. Maximum stability of the azo form should be obtained when the two rings are coplanar, whereas this is not a requirement in the hydrazone tautomer.[33,34] Thus, the hydrazone form could assume a more favorable conformation in the water cavity that results in a lower free energy of the system. Whether the conformational argument is correct or not, the thermodynamic parameters in Table II show that in water, conversion of the azo tautomer to hydrazone is exothermic and is accompanied by increased ordering. This suggests that the solvation cosphere of the hydrazone has greater hydrogen-bonded

(27) J. H. Hildebrand and R. L. Scott, "The Solubility of Nonelectrolytes," Reinhold, New York, N. Y., 1950.
(28) R. B. Hermann, *J. Phys. Chem.*, 76, 2754 (1972).
(29) F. H. Stillinger, *J. Solution Chem.*, 2, 141 (1973).
(30) R. A. Pierotti, *J. Phys. Chem.*, 69, 281 (1965).
(31) T. Förster, *Naturwissenschaften*, 33, 220 (1946).
(32) G. Weber and D. J. R. Laurence, *Biochem. J.*, 51, 31 (1954).
(33) J. A. Barltop and M. Conlong, *J. Chem. Soc. B*, 1081 (1967).
(34) J. E. Kuder, *Tetrahedron*, 28, 1973 (1972).

structure than that of the azo form. The creation of this cosphere is favored in water or water-like solvents or in the water-rich compositions of the aqueous binaries. In water–alcohol mixtures, $\Delta H°$ becomes negligibly small in compositions where little solvent structure remains and $\Delta G°_T$ is governed only by $\Delta S°$.

Whereas the breaks in the plots of $\Delta G°_T$ for PND and of $\bar{\nu}_{max}$ of TNS against the mole fraction of alcohol must result from changes in the solvent structure, we cannot be certain what that structural change is. The fact that so many properties of these mixtures and of solutes dissolved in them show extrema at 4–6 mol % *tert*-butyl alcohol and 10–15 mol % ethanol has led Franks[21] and Arnett[22] to propose that addition of the alcohols to water leads initially to increased structuring and that the extrema appear at compositions where further addition of alcohol caused breakdown of structure. Yaacobi and Ben-Naim[35] interpret the thermodynamics of solution of methane and ethane in ethanol–water mixtures in terms of reinforcement of water structure by ethanol only up to about 3 mol %, with a decrease in water structure between 3 and 20 mol %. By this interpretation, water structure is no longer important above 20 mol %. Proton chemical shift data show that addition of alcohol to water enhances hydrogen-bonded structure between 0 and 5 mol % *tert*-butyl alcohol[36,37] and 0 and 8 mol % ethanol.[38]

If it is assumed that alcohol–water mixtures containing more than 20 mol % ethanol and 6 mol % *tert*-butyl alcohol are unstructured, changes in the values of $\bar{\nu}_{max}$ for TNS and log K_T for PND in the unstructured compositions can be used to estimate the importance of solvent changes such as polarity on the probe properties. The excess changes observed in the water-rich compositions then give an estimate of the contribution of structural factors to the total change. Using the values of $\bar{\nu}_{max}$ for TNS and 1,7-ANS in ethanol–water shown in Figure 4 and extrapolating to 0 and 100% ethanol, we estimate contributions of 4.0 and 2.8 kcal/mol, respectively, to the total change in transition energy from solvent effects not related to structuring. The contributions associated with solvent structuring in this medium are 6.3 kcal/mol for TNS and 4.8 kcal/mol for 1,7-ANS. Using eq 6 and 7 to obtain similar extrapolated values of log K_T of PND in ethanol–water and *tert*-butyl alcohol–water, we estimate contributions to the total change in $\Delta G°_T$ of 1.6 kcal/mol from factors related to structuring and 2.7 kcal/mol from factors not related to structuring in ethanol–water mixtures. The corresponding contributions in *tert*-butyl alcohol–water are 2.0 and 1.9 kcal/mol, respectively. The estimates of contributions to the solvent effects due to the existence of solvent structure may be high, since properties of these mixtures that are related to polarity are not linear functions of mole fraction.

The anomalous solvent effect of TFE on both probes shows that in certain favorable cases, a hydrogen-bonding solvent can interact with dye solute by direct hydrogen bonding. The relatively high acidity and low basicity of the fluorinated alcohols reduce their self-association compared to the hydrocarbon alcohols[39] and thus increase their tendency to solvate dyes[24] and salts[25] by hydrogen bonding. The fact that $\bar{\nu}_{max}$ values of TNS in the hydrocarbon alcohols are correlated by δ and that the values for these alcohols fall on the same correlation line with aprotic solvents shows that self-association of the hydrocarbon alcohol dominates the solvent effect, and hydrogen-bonded solvent–dye interactions are not very important. The fact that a direct hydrogen-bonded interaction with the probes can shift their properties in the same direction as the indirect solvent–solvent hydrogen-bonding interaction may lead to confusing interpretations and emphasizes the importance of examining a wide range of solvent types and properties. It is most important in interpreting solvent effects to examine solvents in which there are not cross correlations between solvent properties, as is the case in many alcohol–water mixtures.

(35) M. Yaacobi and A. Ben-Naim, *J. Solution Chem.*, **2**, 425 (1973).
(36) R. G. Anderson and M. C. R. Symons, *Trans. Faraday Soc.*, **65**, 2550 (1969).
(37) D. N. Glew, H. D. Mak, and N. S. Rath, *Chem. Commun.*, 264 (1968).
(38) J. R. Kuppers and N. E. Carriker, *J. Magn. Resonance*, **5**, 73 (1971).
(39) J. E. Berger, L. R. Dawson, and H. C. Akstran, *J. Phys. Chem.*, **64**, 1458 (1960).

Communications to the Editor

Derivation of (+)- and (−)-C_{17}-Juvenile Hormone from Its Racemic Alcohol Derivative *via* Fungal Metabolism

Sir:

In our metabolic studies with *Helminthosporium sativum*, a racemic mixture of 10,11-epoxyfarnesol has been transformed into (−)-10,11-dihydroxyfarnesoic acid,[1] which was then chemically converted into an enantiomeric pair of C_{16}-juvenile hormone (JH).[2] Novel trans and cis hydration mechanisms of the racemic epoxide were also investigated.[3] These results can be utilized for optical resolution of racemic epoxy isoprenoids, which is difficult to carry out by the usual resolution methods. In this communication, we describe a derivation of an enantiomeric pair of C_{17}-JH from its racemic alcohol derivative *via* fungal metabolism. The difference of the metabolic processes between the enantiomers of 10,11-epoxyhomofarnesol is also shown, being compared with those of 10,11-epoxyfarnesol.

Racemic C_{17}-JH has been synthesized in fairly large

(1) Y. Suzuki and S. Marumo, *Chem. Commun.*, 1199 (1971); *Tetrahedron Lett.*, 1887 (1972).
(2) Y. Suzuki, K. Imai, S. Marumo, and T. Mitsui, *Agr. Biol. Chem.*, 36, 1849 (1972).
(3) Y. Suzuki, K. Imai, and S. Marumo, *J. Amer. Chem. Soc.*, 96, 3703 (1974).